



Adsorptive removal of malachite green from aqueous solution using modified peanut shell

Jiao Li*, Wei Zhang

Department of Material Chemistry, School of Materials Science and Engineering, Shandong University of Technology, Zibo 255049, P.R. China

Tel./Fax: +86 533 2782232; email: zbjli2012@163.com

Received 5 September 2012; Accepted 17 December 2012

ABSTRACT

The aim of the present work is to investigate the adsorptive removal of malachite green (MG) from aqueous solution using modified peanut shell (MPS). The MPS characterizations were investigated using scanning electron microscopy (SEM) and Fourier transform infrared spectra (FTIR). The effect of various factors, such as initial dye concentration, contact time, pH, temperature, and dosage, were investigated during a series of batch adsorption experiments. The SEM and FTIR showed that some components of raw peanut shell (RPS) had been removed during the chemical modification, and many cavities of various dimensions were clearly evident on the surface of MPS. Adsorption experiments showed that MG adsorption uptake was increased with an increase in initial concentration, contact time, solution temperature, and adsorbent dosage. Furthermore, neutral pH was optimum for the removal of MG. The adsorption of MG onto MPS agreed well with the nonlinear Langmuir and Sips isotherm models. The monolayer capacity (q_{\max}) was 32.73 or 35.85 mg/g as calculated from Langmuir or Sips isotherm models, respectively. The adsorption kinetic studies showed that the adsorption process followed the pseudo-second-order kinetic model with a multi-step diffusion process.

Keywords: Peanut shells; Malachite green (MG); Adsorption; Isotherm; Kinetics

1. Introduction

Malachite green (MG), a member of the triphenylmethane group, is extensively used in the aquaculture industry as a biocide. It is also used as a food coloring agent, food additive, a medical disinfectant, and a basic dye in wool, cotton, paper, jute, silk, leather, and acrylic industries for coloring purposes [1,2]. Despite its extensive use, MG dye consists of toxic properties which are known to cause diseases like eye burns, fast breathing, profuse sweating, and cancer of different parts of the body [3,4]. Therefore, its removal

from industrial wastewater before their discharge is essential for environmental safety.

During the last decade, many investigators have presented some methods for the removal of dyes from wastewater such as coagulation [5], membrane filtration [6], biological treatment [7], adsorption [8,9], and photochemical degradation [10,11]. Among all these methods, adsorption has become the most popular technique because of its effectiveness, operational simplicity, low cost, and low energy requirements. Many different types of adsorbents are used to remove various dyes from aqueous effluent such as fly ash [12], volcanic mud [13], clay [14], silica [15], chitin [16,17], and some agricultural waste materials [18,19].

*Corresponding author.

Peanut shell is an abundant and inexpensive agricultural by-product of peanut. China ranks first in peanut production in the world and a potential of 4.5 million tons of peanut shells are produced annually [20]. However, as an agricultural waste material, most of the peanut shells are either burned for energy or abandoned, resulting in a tremendous waste of natural resources and environmental pollution. Therefore, finding uses for peanut shells, especially on an industrial scale, will be beneficial from environmental and economical points of view. Recently, there have been several reports that peanut shells could be modified or converted into activated carbon, and used to remove various metal ions from wastewater, such as Cu^{2+} [21], Cr^{3+} [21], Hg^{2+} [22], Cd^{2+} [22], Pb^{2+} [23], and Cr^{6+} [24]. However, to the best of our knowledge, few investigations are available in the literature about the removal of dyes from wastewater using peanut shells [25].

The aim of the present work is to investigate the possibility of using modified peanut shell (MPS) for the adsorptive removal of MG from aqueous solution. The MPS characterizations were investigated using scanning electron microscopy (SEM) and Fourier transform infrared spectra (FTIR). The effect of various factors such as initial dye concentration, contact time, pH, and temperature were also investigated during a series of batch adsorption experiments. Based on the data on the effects of process parameters, the reaction thermodynamics and kinetics for the adsorption were further discussed.

2. Materials and methods

2.1. Materials

Raw peanut shells (RPSs) used in this study were collected from a local market in Zibo (City in Shandong province, China). The collected peanut shells were extensively washed in running tap water for about 1 h to remove soil and dust, and then washed with distilled water several times. The washed peanut shells were dried at 110°C for 24 h and then crushed into powder and sieved into 36 meshes (about 0.5 mm). The dye MG was purchased from Sigma Aldrich (USA) and used without further purification. The molecular structure of MG is shown in Fig. 1. Other agents used were all analytical grade and all solutions were prepared with distilled water.

2.2. The modification of peanut shells

The MPS were prepared using the following method, 5.0 g crushed peanut shells were mixed with 200 mL of Na_2CO_3 solution (1.0 mol/L) and 5 mL of

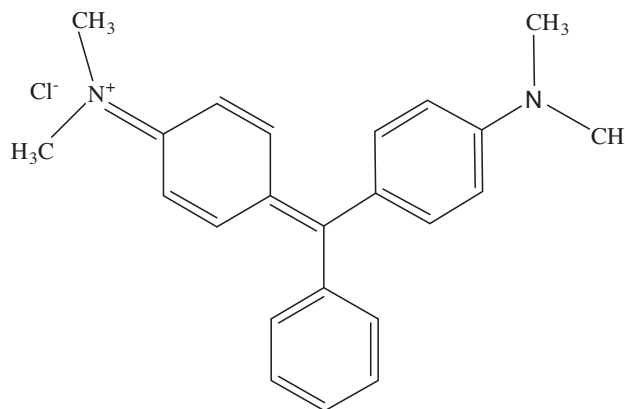


Fig. 1. Structure of MG (molecular formula: $\text{C}_{23}\text{H}_{25}\text{N}_2\text{Cl}$).

epichlorohydrin at 60°C for 10 h. The mixture was then filtered, rinsed with water, oven-dried and stored in a desiccator. The obtained mixture was then filtrated with a 100-mesh stainless screen, rinsed with distilled water for three times, oven-dried at 65°C for 12 h and stored in a desiccator for use. (Peanut shell before and after modification were marked RPS and MPS, respectively).

2.3. Characterization

The surface morphology of peanut shells was carried out by SEM (FEI Sirion 200, NLD). Before the observation, the samples were stabilized on aluminum stubs with adhesive and were sputter-coated with an approximate 100 \AA layer of gold with a vacuum evaporator. This is done to prevent the accumulation of static electric fields at the specimen due to the electron irradiation required during imaging. Another reason for coating, even when there is more than enough conductivity, is to improve contrast. The molecular structure analyses of all the samples were carried out with FTIR (Nicolet 5,700, USA) with the wave numbers recorded from 400 to $4,000 \text{ cm}^{-1}$ at a 1 cm^{-1} resolution. All the measurements were performed at room temperature.

2.4. Adsorption experiments

Adsorption experiments were carried out in 100-mL glass-stoppered, Erlenmeyer flasks containing a fixed amount of adsorbent with 20 mL dye solution at a known initial concentration. The flasks were agitated in a thermostated shaker (SHZ-92A, CHI) with a shaking of 120 rpm. The influence of pH (1.0–10.0), contact time (5.0–240.0 min), initial dye concentration (50, 100, 200, 300, and 400 mg/L), temperature (25, 30, 35, 40, and 45°C), and adsorbent dosage (0.10, 0.15, 0.20, 0.25, 0.30,

0.35, 0.40, 0.45, and 0.50 g/20 mL) were evaluated during the present study. All samples were withdrawn from the shaker, and the dye solution was separated from the adsorbent by centrifugation at 4,500 rpm for 20 min. The absorbencies of solution were measured using a double beam UV-Visible spectrophotometer (Model TU-1901, CHI) at wavelength 617 nm. Then, the concentrations of the solutions were determined by using linear regression equation ($y = 0.0875x + 0.0086$, $R^2 = 0.9994$ (0.1–1 mg/L); $y = 0.1092x - 0.0189$, $R^2 = 0.9997$ (1–10 mg/L)) obtained by plotting a calibration curve for dye over a range of concentrations. All experiments were conducted in triplicate. Then, the amount of MG adsorbed (mg/g) was calculated based on the mass balance equation given below:

$$q_e = \frac{(C_0 - C_e) \times V}{W} \quad (1)$$

where q_e is the equilibrium adsorption capacity of the adsorbent in mg/g; C_0 is the initial concentration of MG in the solution in mg/L; C_e is the equilibrium concentration of MG in the solution in mg/L; V is the volume of the solution in L; and W is the dry weight of MPS in g.

The percentage removal (%) of MG was calculated using the following equation:

$$\text{removal (\%)} = \frac{C_0 - C_e}{C_0} \times 100\% \quad (2)$$

2.5. Adsorption isotherm

The adsorption isotherm indicates how the adsorption molecules distribute between the liquid phase and the solid phase when the adsorption process reaches an equilibrium state. Generally, linear regression is used to determine the most fitted isotherm. However, linear fitting is not a proper way to model adsorption isotherms and can lead to wrong set of parameters [26,27]. Thus, in the present study, the nonlinear Langmuir, Freundlich, and Sips isotherm models were tested to fit the experimental equilibrium data for MG adsorption at 30 °C, respectively.

Langmuir isotherm [28]:

$$q_e = \frac{bQC_e}{1 + bC_e} \quad (3)$$

Freundlich isotherm [29]:

$$q_e = K_F C_e^{1/n} \quad (4)$$

where C_e is the equilibrium concentration of dye in the solution (mg/L), q_e is the amount of adsorbate adsorbed per unit mass of adsorbent (mg/g), Q is the amount of dye adsorbed at complete monolayer (mg/g), b is Langmuir constant related to the affinity of binding sites (L/mg), and a is the measure of the energy of adsorption. The parameters K_F and n are Freundlich constants which can be regarded roughly, the capacity and intensity of adsorption, respectively.

Sips isotherm [30]:

$$q_e = \frac{q_m(b_s C_e)^{1/n}}{1 + (b_s C_e)^{1/n}} \quad (5)$$

where q_m is Sips maximum adsorption capacity (mg/g), b_s is Sips equilibrium constant (L/mg), and $1/n$ is Sips model exponent. If the value for $1/n$ is less than one, it indicates that it is a heterogeneous adsorbent, while values closer to or even one indicates that the adsorbent has relatively more homogeneous binding sites.

2.6. Kinetic modeling

Adsorption kinetic models are used to acquire a better understanding of the controlling mechanism of adsorption process. In this study, three models were used to evaluate the experimental data of different initial concentration.

The pseudo-first-order kinetic model [31]:

$$\log(q_e - q_t) = \log q_e - \frac{k_1 t}{2.303} \quad (6)$$

where q_e and q_t are the amounts of dye adsorbed per unit of adsorbent (mg/g) at equilibrium and at time t , respectively. The symbol k_1 is the pseudo-first-order rate constant (min^{-1}), and t is the contact time (min).

The pseudo-second-order kinetic model [32]:

$$\frac{t}{q_t} = \frac{1}{k_2 q_e^2} + \frac{t}{q_e} \quad (7)$$

where k_2 ($\text{g mg}^{-1} \text{min}^{-1}$) is the rate constant of pseudo-second-order kinetic model for adsorption. The initial adsorption rate, h ($\text{mg g}^{-1} \text{min}^{-1}$), at $t=0$ is defined as:

$$h = k_2 q_e^2 \quad (8)$$

The Weber and Morris intra-particle diffusion model [33]:

$$q_t = k_{id} t^{1/2} + C \quad (9)$$

where k_{id} is the intra-particle diffusion constant ($\text{mg g}^{-1} \text{min}^{-1/2}$), q_t is the amount of dye adsorbed (mg/g) at time t , and C is the intercept.

3. Results and discussion

3.1. Characterization of MPS

The surface morphology of peanut shells before and after modification is observed by SEM (Fig. 2). It can be seen that the surface of RPS is irregular and has lots of particle-like impurities. However, after chemical modification, the surface morphology becomes more neat and regular. Moreover, as seen in Fig. 2(b), many cavities of various dimensions are clearly evident on the surface of MPS. The presence of cavities indicates that there is a large exposed surface area of MPS, which may be convenient for the dye molecules to penetrate into the lignocellulosic structure and interact therein with the surface groups.

The FTIR spectrometry has been widely used to study structural changes in polymers and polymer complexes. Fig. 3(a) exhibits the FTIR spectra of RPS and MPS in the region of $4,000\text{--}400\text{ cm}^{-1}$.

The FTIR spectrum of RPS is identified in Refs. [23,34–36]. A wide and strong --OH stretching band observed between $3,300$ and $3,400\text{ cm}^{-1}$ is ascribed to the presence of polyphenols, luteolin, cellulose, and hemicellulose. Also, this broad band related with hydrogen bonding verifies that water is still remaining in the samples. The absorption band at $1,736.6\text{ cm}^{-1}$ is ascribed to the stretching vibrations of carboxyl groups on the edges of layer planes or to conjugated carbonyl groups (C=O in carbonyls, luteolin or lactones groups). Stretching absorption band at $1,638.1\text{ cm}^{-1}$ is assigned to C=C present in olefinic vibrations in aromatic region. Absorption bands at $1,462.6$, $1,423.7$, and $1,374.3\text{ cm}^{-1}$ are assigned as C-H bending vibrations that show the presence of luteolin, sugar, cellulose, and hemicellulose. Two strong bands

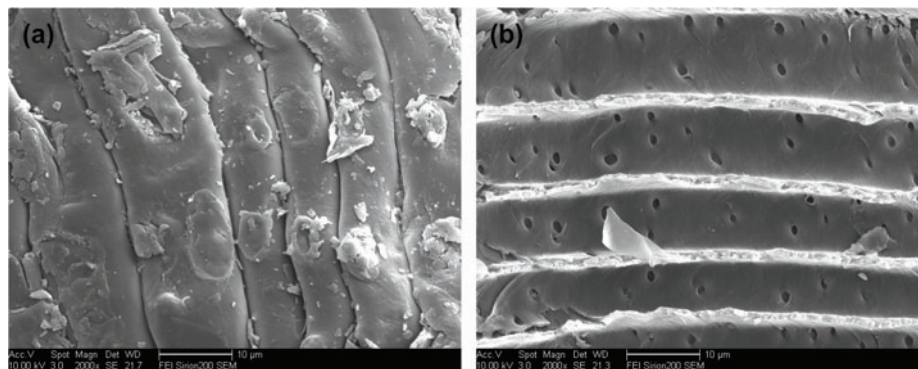


Fig. 2. SEM morphologies of (a) RPS and (b) MPS.

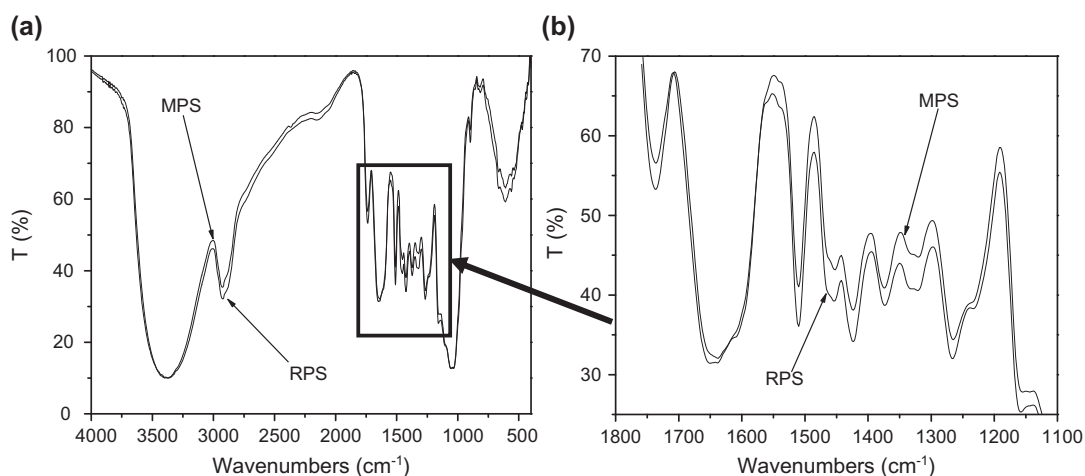


Fig. 3. FTIR spectra of RPS and MPS.

observed at 1,265.2 and 1,051.2 cm^{-1} are assigned to C–O–C and C–O–(H) stretching vibrations, respectively, present in luteolin, cellulose, and hemicellulose.

Fig. 3(a) also shows the FTIR spectra of MPS. It can be observed that the characteristic peaks of MPS are the same as those of RPS, which indicates that the main chemical structure of peanut shells is not changed through the modification reactions mentioned earlier in the method section. However, the slight decrease in the intensities of some adsorption bands (Fig. 3(b)), indicates that some components, such as polyphenols, carboxylic acids, and luteolin, have been removed during the chemical treatment [34].

3.2. Effect of pH on MG adsorption

To study the influence of pH on the adsorption of MG on MPS, the experiments were performed at 300 mg/L initial dye concentration with 0.40 g adsorbent mass at 30 °C for 150 min equilibrium time. It can be seen from Fig. 4 that the adsorption capacity increases significantly from 5.27 to 14.56 mg/g when pH of dye solution increases from 1.0 to 7.0. The increase of the adsorption capacity is likely to be due to two reasons: ① As the number of positively charged surface sites increases with a decrease in the solution pH, the electrostatic repulsion between the positively charged dye MG and the surface of the MPS is higher, which may result in the decreases of dye adsorption [37,38] and ② At lower pH, the presence of excess H^+ ions competing with dyes ions

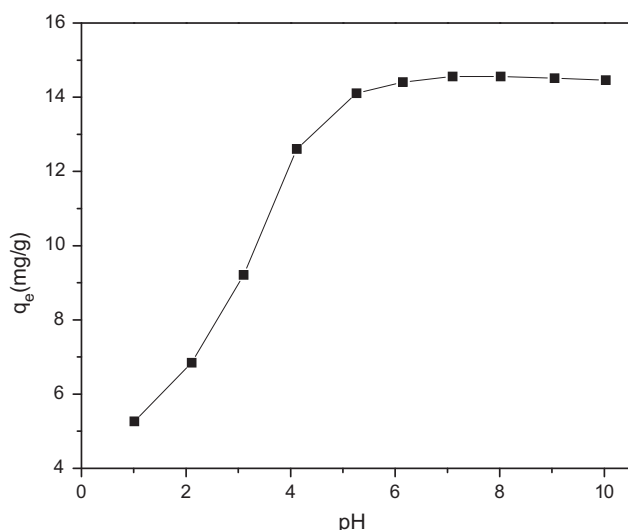


Fig. 4. Effect of pH on MG adsorption by MPS (adsorption experiments: dye concentration: 300 mg/L; sample dose: 0.4 g/20 mL; temperature: 30 °C; and equilibrium time: 150 min).

for the adsorption sites of adsorbent may also decrease the adsorption of MG [39]. These, however, do not explain the slight decrease of dye adsorption at higher pH values ($\text{pH} > 7$). This might be due to the interaction between cationic MG and the hydroxyl ions in the aqueous solution, which is still an assumption and needs to be further studied.

3.3. Effect of temperature on MG adsorption

Fig. 5 shows the effect of temperature on adsorption of MG onto MPS at pH 7.0 and initial dye concentration 300 mg/L. It is clear that the MG uptake slightly increases as the temperature increases indicating better adsorption at higher temperatures, i.e. endothermic process. The adsorption capacity of MG on MPS increases from 14.52 to 15.01 mg/g, with an increase of temperature from 25 to 45 °C. At higher temperature, more dye molecules have sufficient energy to undergo an interaction with active sites at the adsorbent surface. Moreover, the enhanced mobility of MG from the bulk solution towards the adsorbent surface shall be taken into account [40].

3.4. Effect of adsorbent dosage on MG adsorption

The effect of adsorbent dosage on the uptake of MG is shown in Fig. 6. This figure reveals that adsorption of MG increases with increasing amount of MPS (0.10–0.40 g/20 mL) and remains almost constant after increasing up to a certain limit (≥ 0.40 g/20 mL).

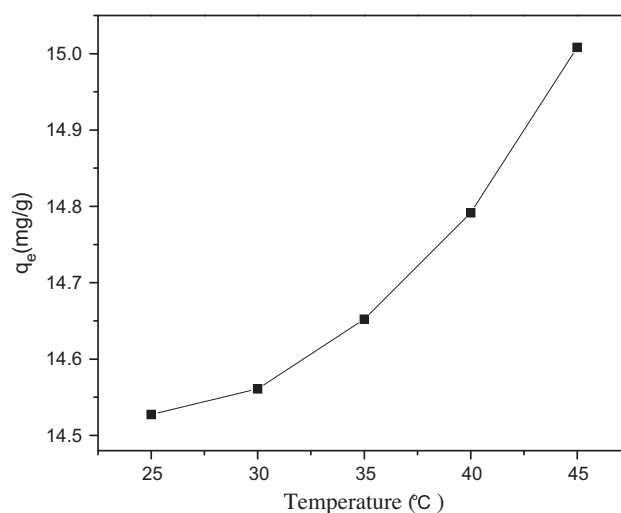


Fig. 5. Effect of the temperature on MG adsorption by MPS (adsorption experiments: dye concentration: 300 mg/L; sample dose: 0.4 g/20 mL; pH: 7.0; and equilibrium time: 150 min).

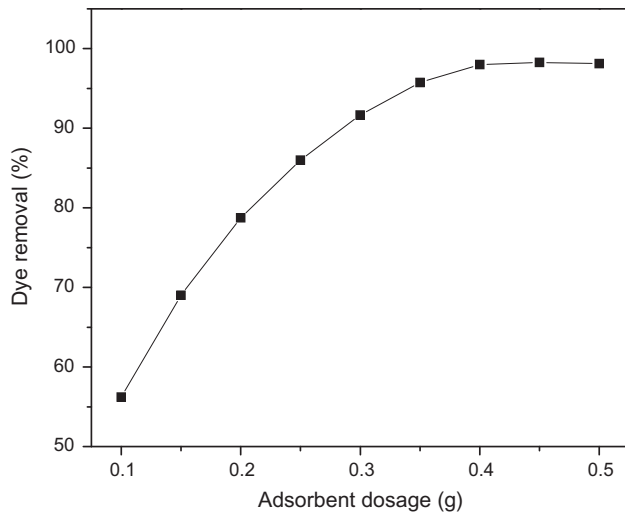


Fig. 6. Effect of adsorbent dosage on MG adsorption by MPS (adsorption experiments: dye concentration: 300 mg/L; temperature: 30°C; pH: 7.0; and equilibrium time: 150 min).

This can be attributed to greater adsorbent surface area and availability of more adsorption sites resulting from the increased dose of the adsorbent, as already reported [41]. The optimum dosage is found to be 0.40 g/20 mL, as the dye removal is 98.02%.

3.5. Effect of contact time and initial concentration on MG adsorption

Fig. 7 shows plots of adsorption capacity of MG onto MPS vs. contact time for different initial MG concentrations. As can be seen from Fig. 7, the amount

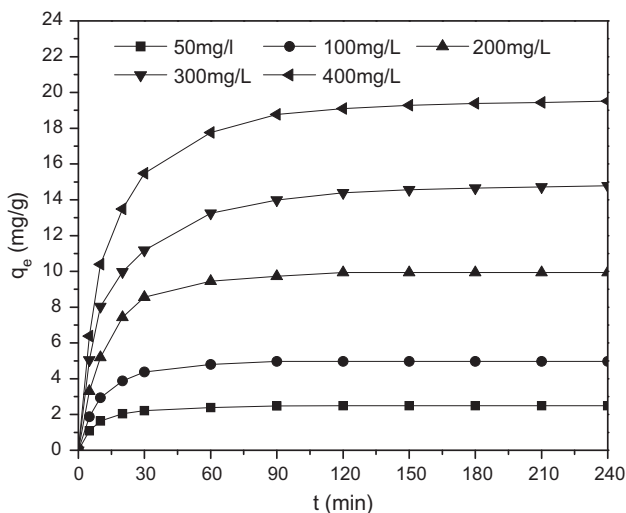


Fig. 7. Effect of contact time and initial concentration on MG adsorption by MPS (adsorption experiments: sample dose: 0.4 g/20 mL; pH: 7.0; and temperature: 30°C).

of the adsorbed dye at low initial concentration (≤ 100 mg/L) achieve adsorption equilibrium in about 60 min, while at high initial dye concentration (≥ 300 mg/L), the time necessary to reach equilibrium is about 150 min. These results indicate that the adsorption equilibrium time is much higher at high initial dye concentration than that at low initial concentration. Moreover, it can be found from Fig. 7 that the MG adsorption capacity is improved with increased initial dye concentrations. The adsorption capacity for 150 min with initial dye concentration at 400 mg/L is 674.73% greater than that at 50 mg/L. This might be explained by the fact that a higher initial dye concentration led to an increase in the mass gradient between the solution and MPS, which then functions as a driving force for the transfer of dye molecules from the bulk solution to the adsorbent surface.

3.6. Adsorption isotherms

Langmuir model is based on the assumption that adsorption energy is constant and independent of surface coverage. The maximum adsorption occurs when the surface is covered by a monolayer of adsorbate [28]. Freundlich model is based on sorption on a heterogeneous surface of varied affinities [29]. While Sips model is an additional empirical model which has the features of both Langmuir and Freundlich isotherm models [30].

The different isotherm of adsorption of MG onto MPS is performed, using the best experimental conditions described previously (see Fig. 8). The obtained values for Langmuir, Freundlich, and Sips

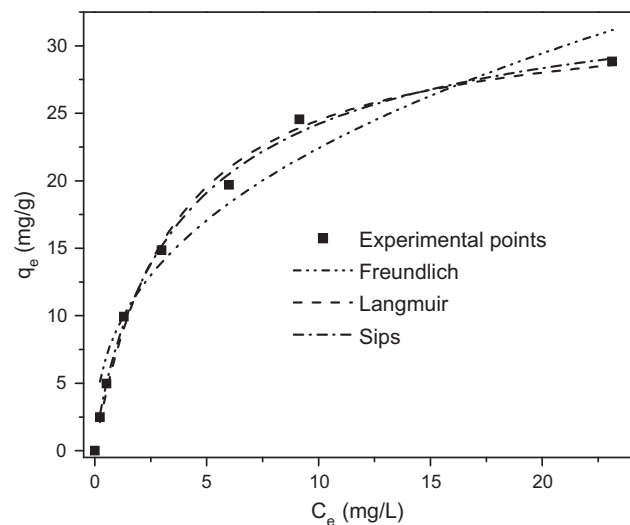


Fig. 8. Nonlinear isotherm fittings at 30°C for the adsorption of MG onto MPS.

Table 1
Isotherm parameters for the adsorption of MG onto MPS at 30°C

Isotherm model		Adsorbent (MPS)
Langmuir isotherm	Q (mg/g)	32.73
	b (L/mg)	0.30
	R^2	0.9928
	χ^2	0.70
Freundlich isotherm	k_F	9.06
	$1/n$	2.54
	R^2	0.9437
	χ^2	5.51
Sips isotherm	q_m (mg/g)	35.85
	b_s (mL/g)	0.23
	$1/n$	0.86
	R^2	0.9949
	χ^2	0.50

isotherm constants, the correlation coefficients (R^2), and chi-square test statistic (χ^2) are listed in Table 1. These values of R^2 and χ^2 are regarded as a measure of the goodness-of-fit of experimental data on the isotherm models.

As shown in Fig. 8, Langmuir and Sips isotherm models exhibited a slightly better fit to the experimental data than Freundlich isotherm model. Moreover, the results of R^2 and χ^2 for Langmuir and Sips isotherm model (Table 1) indicated that Sips isotherm model appeared to be the best fitting model for the adsorption isotherm data of MPS because it displayed the highest R^2 (0.9949) and the lowest χ^2 (0.50) values. The value of

exponent $1/n$ for Sips isotherm model is less than one for MPS indicating that it is a heterogeneous adsorbent. These suggest the monolayer coverage of MG onto treated peanut shells surface as well as the heterogeneous distribution of active sites on the MPS surface. The monolayer capacity (q_{max}) is 32.73 or 35.85 mg/g, as calculated from Langmuir or Sips models, respectively.

3.7. Adsorption kinetics

The straight-line plots of $\log(q_e - q_t)$ vs. t (Fig. 9(a)) for the pseudo-first-order reaction and t/q_t vs. t (Fig. 9(b)) for the pseudo-second-order reaction of the adsorption MG onto MPS had been investigated to obtain the rate parameters. Values of $q_{e,r}$, k_1 , h , and k_2 and correlation coefficients R_1^2 and R_2^2 of MG under different conditions were calculated from these plots and shown in Table 2.

It can be seen that the corresponding linear regression correlation coefficient values of the pseudo-second-order kinetic model are over 0.9995 for all concentrations, and the $q_{e,cal}$ values obtained from this model also agree with the experimental $q_{e,exp}$ values at different initial MG concentrations. These results suggest that the pseudo-second-order kinetic model is more valid to describe the adsorption behavior of MG onto MPS compared to the pseudo-first-order model. The better fit with pseudo-second-order model implies the adsorption process is interaction-controlled, with chemisorptions involved. Similar phenomena were observed for MG adsorption onto *Luffa* cylindrical [42] and pine wood decayed by *fungi Poria cocos* [43].

The intra-particle diffusion model based on the theory proposed by Weber and Morris [33] is widely used to predict the rate controlling step. According to

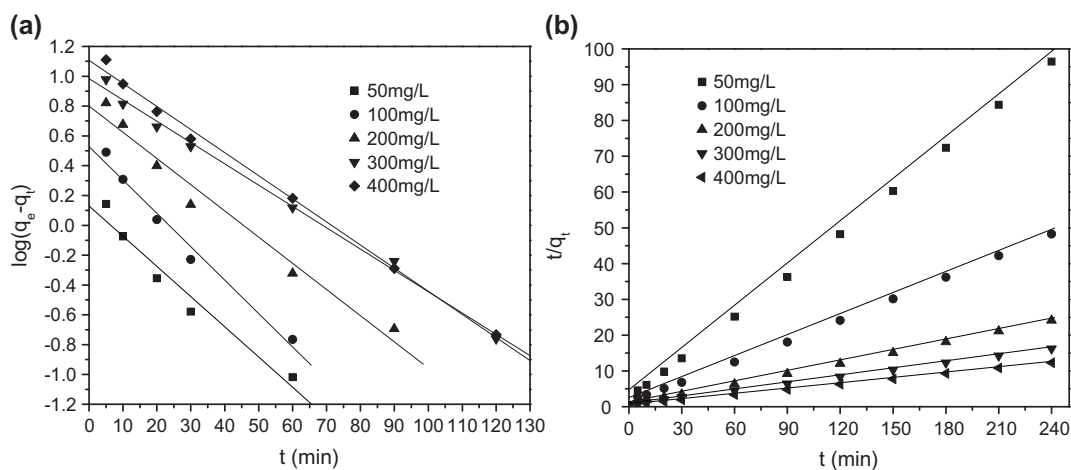


Fig. 9. Regressions of kinetic plots different initial concentrations (a) pseudo-first-order model and (b) pseudo-second-order model.

Table 2
Adsorption kinetic parameters for the adsorption of MG onto MPS at different initial concentrations

C_0 (mg/L)	$q_{e, \text{exp}}$ (mg/g)	Pseudo-first-order model			Pseudo-second-order model			
		q_e (mg/g)	k_1 (min^{-1})	R_1^2	q_e (mg/g)	k_2 (g/mg min)	R_2^2	h (mg/g min)
50	2.39	1.35	0.05	0.9577	2.55	0.06	0.9998	0.52
100	4.80	3.38	0.05	0.9823	5.12	0.03	0.9996	0.79
200	9.73	6.31	0.04	0.9727	10.35	0.01	0.9995	1.07
300	14.56	9.64	0.03	0.9950	15.46	0.01	0.9998	2.39
400	19.28	12.79	0.04	0.9856	20.40	0.01	0.9999	4.12

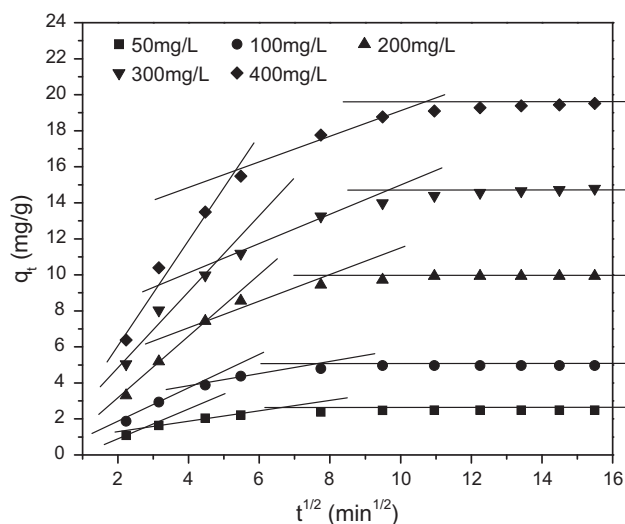


Fig. 10. Weber–Morris intra-particle diffusion plots for the adsorption of MG by MPS.

this model, if the regression of q_t vs. $t^{1/2}$ is linear and passes through the origin, then the rate of adsorption is controlled by intra-particle diffusion for the entire adsorption period [44]. Fig. 10 shows the intra-particle diffusion plots of MG adsorption on MPS. It is clear that the plots are multi-linear, containing at least three linear segments. This result illustrates that multiple stages are involved in the adsorption process [13]. The first sharper portion is attributed to the diffusion of adsorbate through the solution to the external surface of adsorbent or the boundary layer diffusion of solute molecules. The second portion describes the gradual layer adsorption stage, where intra-particle diffusion is rate-controlled. The third portion is attributed to the final equilibrium stage of adsorption, where the intra-particle diffusion starts to slow down because most of the adsorption sites are saturated. These multi-linear curves may result from the adsorption on the nonuniform dimension cavities in the steps and irregular edges of MPS, as shown by the SEM photographs in Fig. 2(b).

4. Conclusion

The present study investigated the adsorption of MG from aqueous solutions by using an adsorbent of peanut shells modified with sodium carbonate and epichlorohydrin. The SEM and FTIR showed that some components of RPS had been removed during the treatment, and many cavities of various dimensions were clearly evident on the surface of peanut shells. Batch adsorption experiments showed that the MG dye adsorption process was dependent on initial pH value of the dye solution, temperature, adsorbent dosage, contact time, and initial dye concentration. The adsorption of MG onto MPS agreed well with the nonlinear Langmuir and Sips isotherm models, and the best-fit adsorption isotherm was achieved with Sips model. The monolayer capacity (q_{max}) was 32.73 or 35.85 mg/g, as calculated from Langmuir or Sips isotherm models, respectively. The adsorption kinetic studies showed that the adsorption process followed the pseudo-second-order kinetic model with a multi-step diffusion process. Taking into consideration all the above obtained results, it can be concluded that MPS should be a promising and low-cost adsorbent for the removal of MG in industrial wastewater treatment.

Acknowledgments

This work was financed by the Natural Science Foundation of Shandong Province (No. ZR2011EL033) and the Scientific Research Foundation from Shangdong University of Technology (No. 410010).

References

- [1] Z.Y. Guo, P.P. Gai, T.T. Hao, J. Duan, S. Wang, Determination of malachite green residues in fish using a highly sensitive electrochemiluminescence method combined with molecularly imprinted solid phase extraction, *J. Agric. Food Chem.* 59 (2011) 5257–5262.
- [2] Y.C. Sharma, Adsorption characteristics of a low-cost activated carbon for the reclamation of colored effluents containing malachite green, *J. Chem. Eng. Data.* 56 (2011) 478–484.

- [3] F. Ding, X.N. Li, J.X. Diao, Y. Sun, L. Zhang, L. Ma, X.L. Yang, L. Zhang, Y. Sun, Potential toxicity and affinity of triphenylmethane dye malachite green to lysozyme, *Ecotoxicol. Environ. Saf.* 78 (2012) 41–49.
- [4] S. Srivastava, R. Sinha, D. Roy, Toxicological effects of malachite green, *Aquat. Toxicol.* 66 (2004) 319–329.
- [5] Z. Khalili, B. Bonakdarpour, Statistical optimization of anaerobic biological processes for dye treatment, *Clean Soil Air Water* 38 (2010) 942–950.
- [6] D. Mahanta, G. Madras, S. Radhakrishnan, S. Patil, Adsorption of sulfonated dyes by polyaniline emeraldine salt and its kinetics, *J. Phys. Chem. B* 112 (2008) 10153–10157.
- [7] A.R. Khataee, G. Dehghan, Optimization of biological treatment of a dye solution by macroalgae *Cladophora* sp. using response surface methodology, *J. Taiwan Inst. Chem. Eng.* 42 (2011) 26–33.
- [8] M. Rafatullah, O. Sulaiman, R. Hashim, A. Ahmad, Adsorption of methylene blue on low-cost adsorbents: A review, *J. Hazard. Mater.* 177 (2010) 70–80.
- [9] I. Acar, A. Bal, G. Güçlü, Adsorption of basic dyes from aqueous solutions by depolymerization products of post-consumer PET bottles, *Clean Soil Air Water* 40 (2012) 325–333.
- [10] W. Chen, W. Lu, Y. Yao, M. Xu, Highly efficient decomposition of organic dyes by aqueous-fiber phase transfer and *in situ* catalytic oxidation using fiber-supported cobalt phthalocyanine, *Environ. Sci. Technol.* 41 (2007) 6240–6245.
- [11] M.A. Nawi, S.M. Zain, Enhancing the surface properties of the immobilized Degussa P-25 TiO₂ for the efficient photocatalytic removal of methylene blue from aqueous solution, *Appl. Surf. Sci.* 258 (2012) 6148–6157.
- [12] P. Hareesh, K.B. Babitha, S. Shukla, Processing fly ash stabilized hydrogen titanate nano-sheets for industrial dye-removal application, *J. Hazard. Mater.* 229–230 (2012) 177–182.
- [13] A.A. Jalil, S. Triwahyono, S.H. Adam, N.D. Rahim, M.A.A. Aziz, N.H.H. Hairom, N.A.M. Razali, M.A.Z. Abidin, M.K.A. Mohamadiah, Adsorption of methyl orange from aqueous solution onto calcined Lapindo volcanic mud, *J. Hazard. Mater.* 181 (2010) 755–762.
- [14] Y.C. Lee, E.J. Kim, J.W. Yang, H.J. Shin, Removal of malachite green by adsorption and precipitation using aminopropyl functionalized magnesium phyllosilicate, *J. Hazard. Mater.* 192 (2011) 62–70.
- [15] M. Anbia, S.A. Hariri, S.N. Ashrafzadeh, Adsorptive removal of anionic dyes by modified nanoporous silica SBA-3, *Appl. Surf. Sci.* 256 (2010) 3228–3233.
- [16] W.A. Morais, A.L.P. Fernandes, T.N.C. Dantas, M.R. Pereira, J.L.C. Fonseca, Sorption studies of a model anionic dye on crosslinked chitosan, *Colloids Surfaces A: Physicochem. Eng. Aspects* 310 (2007) 20–31.
- [17] W.S. Wan Ngah, N.F.M. Ariff, A. Hashim, M.A.K.M. Hanafiah, Malachite green adsorption onto chitosan coated bentonite beads: Isotherms, kinetics and mechanism, *Clean Soil Air Water* 38 (2010) 394–400.
- [18] M.C. Shih, Kinetics of the batch adsorption of methylene blue from aqueous solutions onto rice husk: Effect of acid-modified process and dye concentration, *Desal. Treat.* 37 (2012) 200–214.
- [19] W. Zhang, H. Li, X. Kan, L. Dong, H. Yan, Z. Jiang, H. Yang, A. Li, R. Cheng, Adsorption of anionic dyes from aqueous solutions using chemically modified straw, *Bioresour. Technol.* 117 (2012) 40–47.
- [20] C.D. Liao, Chemical utilization of peanut shell, *Technol. Develop. Chem. Ind.* 22 (2004) 24–25, (in Chinese).
- [21] Z.A. AL-Othman, R. Ali, M. Naushad, Hexavalent chromium removal from aqueous medium by activated carbon prepared from peanut shell: Adsorption kinetics, equilibrium and thermodynamic studies, *Chem. Eng. J.* 184 (2012) 238–247.
- [22] Y. Liu, X.M. Sun, B.H. Li, Adsorption of Hg²⁺ and Cd²⁺ by ethylenediamine modified peanut shells, *Carbohydr. Polym.* 81 (2010) 335–339.
- [23] X.U. Tao, X.Q. Liu, Peanut shell activated carbon: Characterization, surface modification and adsorption of Pb²⁺ from aqueous solution, *Chin. J. Chem. Eng.* 16 (2008) 401–405.
- [24] A.W. Krowiak, R.G. Szafran, S. Modelski, Biosorption of heavy metals from aqueous solutions onto peanut shell as a low-cost biosorbent, *Desalination* 265 (2011) 126–134.
- [25] M.S. Tanyildizi, Modeling of adsorption isotherms and kinetics of reactive dye from aqueous solution by peanut hull, *Chem. Eng. J.* 168 (2011) 1234–1240.
- [26] K.V. Kumar, S. Sivanesan, Prediction of optimum sorption isotherm: Comparison of linear and non-linear method, *J. Hazard. Mater.* 126 (2005) 198–201.
- [27] B. Subramanyan, A. Das, Linearized and non-linearized isotherm models comparative study on adsorption of aqueous phenol solution in soil, *Int. J. Environ. Sci. Tech.* 6 (2009) 633–640.
- [28] I. Langmuir, The adsorption of gases on plane surfaces of glass, mica and platinum, *J. Am. Chem. Soc.* 40 (1918) 1361–1403.
- [29] H.M.F. Freundlich, Über die adsorption in losungen (Over the adsorption in solution), *Z. Phys. Chem.* 57 (1906) 385–470.
- [30] R.J. Sips, On the Structure of a Catalyst Surface, *J. Chem. Phys.* 16 (1948) 490–495.
- [31] S. Lagergren, About the theory of so-called adsorption of soluble substances, *Kungliga Svenska Vetenskapsakademiens Handlingar* 24 (1898) 1–39.
- [32] Y.S. Ho, G. McKay, Pseudo-second order model for sorption processes, *Process Biochem.* 34 (1999) 451–465.
- [33] W.J. Weber Jr., J.C. Morris, Kinetics of adsorption on carbon from solution, *J. Sanitary Eng. Div. Proceed. Am. Soc. Civil Eng.* 89 (1963) 31–59.
- [34] H.F. Lv, J.P. Zhai, Q. Li, J. Zhou, Effects of acidic formaldehyde treatment of peanut hull on its adsorptive capacities for heavy metals, *Environ. Pollut. Control* 29 (2007) 837–840, (in Chinese).
- [35] E. Apaydin-Varol, A.E. Pütün, Preparation and characterization of pyrolytic chars from different biomass samples, *J. Anal. Appl. Pyrol.* 98 (2012) 29–36.
- [36] H.P. Yang, R. Yan, H.P. Chen, D.H. Lee, C.G. Zheng, Characteristics of hemicellulose, cellulose and lignin pyrolysis, *Fuel* 86 (2007) 1781–1788.
- [37] C.P. Sekhar, S. Kalidhasan, V. Rajesh, N. Rajesh, Bio-polymer adsorbent for the removal of malachite green from aqueous solution, *Chemosphere* 77 (2009) 842–847.
- [38] B.H. Hameed, M.I. El-Khaiary, Batch removal of malachite green from aqueous solutions by adsorption on oil palm trunk fibre: Equilibrium isotherms and kinetic studies, *J. Hazard. Mater.* 154 (2008) 237–244.
- [39] O. Hamdaoui, Batch study of liquid-phase adsorption of methylene blue using cedar sawdust and crushed brick, *J. Hazard. Mater. B* 135 (2006) 264–273.
- [40] R. Ahmad, R. Kumar, Adsorption studies of hazardous malachite green onto treated ginger waste, *J. Environ. Manage.* 91 (2010) 1032–1038.
- [41] G.O. El-Sayed, Removal of methylene blue and crystal violet from aqueous solutions by palm kernel fiber, *Desalination* 272 (2011) 225–232.
- [42] A. Altınışık, E. Gür, Y. Seki, A natural sorbent, *Luffa cylindrica* for the removal of a model basic dye, *J. Hazard. Mater.* 179 (2009) 658–664.
- [43] H. Zhang, Y. Tang, X. Liu, Zh. Ke, X. Su, D. Cai, X. Wang, Y. Liu, Q. Huang, Z. Yu, Improved adsorptive capacity of pine wood decayed by fungi *Poria cocos* for removal of malachite green from aqueous solutions, *Desalination* 274 (2011) 97–104.
- [44] K.G. Bhattacharyya, A. Sharma, Kinetics and thermodynamics of Methylene blue adsorption on neem (*Azadirachta indica*) leaf powder, *Dyes Pigments* 65 (2005) 51–59.